Phase plane analysis of traffic flow based on driver's expected response model

Le Xu[1], *Wenhuan* Ai[1,*] and *Dawei* Liu[2]

[1]College of Computer Science and Engineering, Northwest Normal University, Lanzhou, Gansu, 730070, China
[2]College of Electrical Engineering, Lanzhou Institute of Technology, Lanzhou, Gansu, 730050, China

Abstract. At present, researchers have proposed many traffic flow models and research methods of traffic phenomena, but few of them are analyzed from the perspective of system stability. Therefore, this paper proposes a phase plane analysis method from the perspective of traffic flow stability. This method can describe the nonlinear traffic flow phenomenon on the road from the perspective of system global stability. The nonlinear system of the model is obtained by traveling wave substitution and Taylor expansion, and the equilibrium point of the model is solved by specifying the model parameters. According to the qualitative theory of differential equation, the model is further analyzed to judge the type and stability of equilibrium point. Finally, the simulation diagram is used for numerical verification.

Keywords: Traveling wave solutions, Nonlinear traffic flow phenomena, Traveling wave substitution, Phase plane analysis.

1 Introduction

The macroscopic model of traffic flow [1] [2] adopts Euler's point of view, which regards traffic flow as a compressible continuous fluid medium composed of many vehicles and uses macroscopic quantities such as vehicle density and flow rate to describe traffic flow laws. In numerical simulation, because the macroscopic model focuses on the lumped nature of vehicle flow, the simulation efficiency only depends on the selected numerical format, so it usually has high computational efficiency [3]. The macroscopic continuum model of traffic flow started from the LWR model of Lethilland and Whitham [4] [5], and Richard [6]. The model describes the traffic flow in terms of the average density ρ, the average velocity v and the flow rate q.

In 1995, Bando [7] proposed a classical microscopic model, the optimal velocity model:

$$\frac{dv_n(t)}{dt} = a[v(\Delta x_n(t)) - v_n(t)] \quad (1)$$

* Corresponding author: wenhuan618@163.com

The letter a represents the sensitivity coefficient. Later, Heling and Tile [8] et al improved the Bando model for defects such as large acceleration and unreasonable deceleration. On this basis, Liu [9] and others added the expected effect to study the impact of the driver's expected effect on the whole macro traffic flow and established the macroscopic hydrodynamic model:

$$\frac{\partial v}{\partial t} + [v + aT\rho^2 Ve'(\rho)\Delta]\frac{\partial v}{\partial x} = a[Ve(\rho) - v] - aT\rho^2 Ve'(\rho)\frac{\Delta^2}{2}v_{XX} \tag{2}$$

Based on the theory of phase plane analysis, this paper further studies the type and stability of the equilibrium point of the model considering the driver's expected response. The phase plane analysis is based on the traveling wave solution of the high-order traffic flow model proposed in the Lagrangian coordinate system, which is used to analyze and determine the type and stability of the equilibrium solution.

The rest of this article is organized as follows. In the second section, we discussed the model and its derivation in detail. In the third section, we deduced the balance point type and stability of the model and discussed the classification and stability of the model balance point. In the fourth section, the numerical simulation of specified parameters is performed. The fifth section summarizes the full text.

2 Model and its derivation

We take the driver's expected response model established by Liu [9] to improve bando model as an example to analyze the complex traffic flow phenomenon. The model not only solves the problem of backward propagation in many high-order continuous models, but also can reproduce many complex traffic phenomena observed on the road. The model is composed of the following two equations, a local vehicle number conservation equation and an equation of motion:

$$\frac{\partial \rho}{\partial t} + \frac{\partial(\rho v)}{\partial x} = 0 \tag{3}$$

$$\frac{\partial v}{\partial t} + [v + aT\rho^2 Ve'(\rho)\Delta]\frac{\partial v}{\partial x} = a[Ve(\rho) - v] - aT\rho^2 Ve'(\rho)\frac{\Delta^2}{2}v_{XX} \tag{4}$$

In the equation: $Ve[\rho(x,t)]$——The velocity function is optimized.

Suppose that there are traveling wave solutions $\rho(z)$ and $v(z)$ in the model, where $z = x - ct$ is the traveling wave velocity $c < 0$. by using the above results and substituting them into equations (3) and (4), we can get the following results:

$$-c\rho_z + q_z = 0 \tag{5}$$

$$-cv_z + (v + aT\rho^2 Ve'(\rho)\Delta)v_z = a(V_e - v) + (-aT\rho^2 Ve'(\rho)\frac{\Delta^2}{2})v_{zz} \tag{6}$$

From formula (5):

$$v_z = \frac{c\rho_z}{\rho} - \frac{q\rho_z}{\rho^2} \tag{7}$$

Substitute (7) into equation (6) above, we can get the flowing equation:

$$-\frac{\rho_z}{\rho^3}q^2+\left[\frac{\left(2c+\left(-aT\rho^2Ve'(\rho)\Delta\right)\right)}{\rho^2}\rho_z+\frac{a}{\rho}+\frac{-aT\rho^2Ve'(\rho)\frac{\Delta^2}{2}}{\rho^2}\rho_{zz}\right]q=\frac{\left(c^2+c\left(-aT\rho^2Ve'(\rho)\Delta\right)\right)\rho_z}{\rho}+$$
$$a\,Ve(\rho)+\frac{c\left(-aT\rho^2Ve'(\rho)\frac{\Delta^2}{2}\right)}{\rho}\rho_{zz} \quad (8)$$

In the formula (5), integrate with respect to z:

$$-c\rho+q=const=q_* \quad (9)$$

$$q=q_*+c\rho \quad (10)$$

Then substituting (10) into (8), we can get:

$$\left[\frac{\left(-aT\rho^2Ve'(\rho)\frac{\Delta^2}{2}\right)}{\rho}(q_*+cp)-c\left(-aT\rho^2Ve'(\rho)\frac{\Delta^2}{2}\right)\right]-\rho_{zz}-\left[\frac{(q_*+cp)^2}{\rho^2}-\frac{\left(2c+\left(-aT\rho^2Ve'(\rho)\Delta\right)\right)(q_*+c\rho)}{\rho}+\left(c^2+c\left(-aT\rho^2Ve'(\rho)\Delta\right)\right)\right]\rho_z+a(q_*+c\rho)-a\rho V_e(\rho)=0 \quad (11)$$

Simplify the second order ordinary differential equation about $\rho(z)$:

$$\rho_{zz}-G(\rho,q_*)\rho_z-F(\rho,c,q_*)=0 \quad (12)$$

Among them:

$$G(\rho,q_*)=\frac{1}{\left(-aT\rho^2Ve'(\rho)\frac{\Delta^2}{2}\right)}\left(\frac{q_*}{\rho}-\left(-aT\rho^2Ve'(\rho)\Delta\right)\right) \quad (13)$$

$$F(\rho,c,q_*)=\frac{a\rho}{\left(-aT\rho^2Ve'(\rho)\frac{\Delta^2}{2}\right)q_*}[q_*+c\rho-\rho V_e(\rho)] \quad (14)$$

Let $y=\frac{d\rho}{dz}$, equation (12) can be transformed into a system of first-order ordinary differential equations (or called nonlinear dynamic system):

$$\begin{cases}\frac{d\rho}{dz}=y\\ \frac{dy}{dz}=G(\rho,q_*)y+F(\rho,c,q_*)\end{cases} \quad (15)$$

3 The balance point type and stability of the model

This section mainly discusses the equilibrium point of the model and its stability. If the right end of equation group (15) is zero, y = 0 and F = 0 can be obtained. Thus, the equilibrium point is determined $(\rho_i,0)$. The linear system obtained by Taylor expansion of equation (15) at the equilibrium point is shown in equation (16).

$$\begin{cases}\rho'=y\\ y'=G(\rho_i,q_*)y+F'(\rho_i,c,q_*)(\rho-\rho_i)\end{cases} \quad (16)$$

Therefore, the Jacobian matrix of the system at the equilibrium point can be obtained as:

$$L = \begin{bmatrix} 0 & 1 \\ F_i' & G_i \end{bmatrix} \tag{17}$$

Accordingly, the Jacobian characteristic equation is:

$$\lambda^2 - G_i\lambda - F_i' = 0 \tag{18}$$

Where $G_i = G(\rho_i, q_*)$ and $F_i' = F'(\rho_i, c, q_*)$. From (13) and (14) forms, we can get:

$$F_i' = \frac{\rho_i}{(-aT\rho^2 Ve'(\rho)\frac{\Delta^2}{2})q_*}[c - \rho_i V_e'(\rho_i) - V_e(\rho_i)] \tag{19}$$

$$G_i = \frac{a}{(-aT\rho^2 Ve'(\rho)\frac{\Delta^2}{2})}\left[\frac{q_*}{\rho_i} - (-aT\rho^2 Ve'(\rho)\Delta)\right] \tag{20}$$

According to the qualitative theory of differential equations, the balance point type of linear system (16) can be determined as follows: (a) When $F_i' > 0$, the balance point is a saddle point; (b) When$G_i^2 + 4F_i' > 0$and$F_i' < 0$, the balance point It is a node; (c) When $G_i^2 + 4F_i' < 0$and $G_i \neq 0$, the balance point is the focus; (d) When $F_i' < 0$ and $F_i' < 0$, the balance point is the center. When z→ $\pm\infty$, the stability of the linear system at the saddle point is unstable; when $G_i < 0(G_i > 0)$, the stability at the node and focal point, for $z \to +\infty(z \to -\infty)$ is stable.

From the Hartman-Gorban linearization theorem, we know that the nonlinear system (15) and the linear system (16) have the same equilibrium point. Given any set of traveling wave velocity c and traveling wave parameter q, the equilibrium points $\rho_i(i = 1,2)$ of the linear system (16) can be solved. Select the balance velocity function proposed in [10]:

$$V_e(\rho) = V_f\left\{\left[1 + exp\left(\frac{\rho/\rho_m - 0.25}{0.06}\right)\right]^{-1} - 3.72 \times 10^{-6}\right\} \tag{21}$$

In the model, the parameter values are as follows:$V_f = 30m/s$, ρ_m=0.2veh/m, a=0.1s^{-1}, Δ= 100m, $T = 0.5s$. When $\rho = 0$, this is a trivial balance point and has no practical meaning, so this article only needs to discuss other balance points. From the above discussion and (19)-(20), the type and stability of the equilibrium point can be judged, as shown in Table 1.

Table 1. Types of equilibrium points and their stability when model parameters are given, Δ_i=$G_i^2 + 4F_i', i = 1,2$.

	ρ_1	ρ_2
	0.0938	0.1447
$(c,q_*) = (-1.371,0.2)$	$\Delta_i < 0$, $G_i < 0$, spiral point Stable for $z \to +\infty$ Unstable for $z \to -\infty$	$F_i' > 0$, saddle point Unstable for $z \to \pm\infty$
	0.0223	0.0594
$(c,q_*) = (-1.38,0.64)$	$F_i' > 0$, saddle point Unstable for $z \to \pm\infty$	$\Delta_i < 0$, $G_i < 0$, spiral point Stable for $z \to +\infty$ Unstable for $z \to -\infty$

4 Numerical simulation

The two sets of parameters in Table 1 are selected to simulate the stability of the nonlinear system (15) at the equilibrium point. The phase plane near the equilibrium point is shown in Figure 1. (a)and Figure 1. (b)The balance point is $(\rho_i,0)$, and i =1,2, $\rho_1 < \rho_2$.

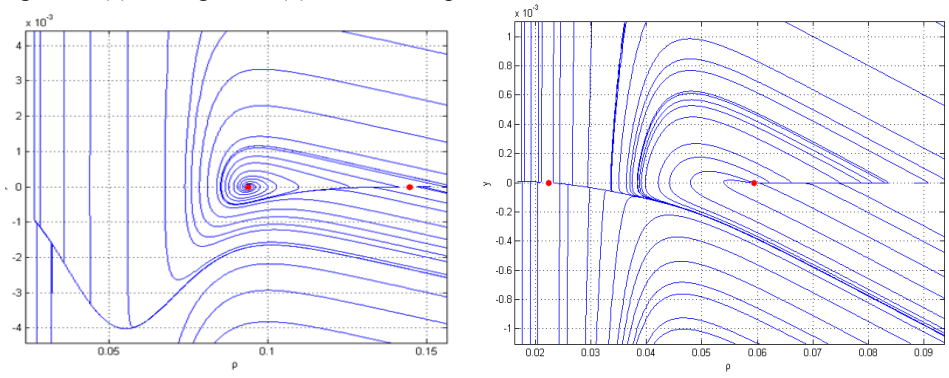

(a) (b)

Fig. 1. Phase plane ρ - y trajectory diagram, (a) where traveling wave velocity $c = -1.371$, traveling wave parameter $q_* = 0.2$.(b) where traveling wave velocity $c = -1.38$, traveling wave parameter $q_* = 0.64$

Figure 1. (a) corresponds to the first case in Table 1. When z→ $\pm\infty$, the system is at the equilibrium point $(\rho_2, 0)$ is unstable, and the nearby tracks are far away from this point. When z→ $+\infty$, several trajectories tend to focus $(\rho_1, 0)$; When z→ $-\infty$, these trajectories are far away from the focus and eventually tend to infinity. It shows that when z→ $\pm\infty$, the system is stable at $(\rho_1, 0)$; when z→ $-\infty$, the system is unstable at $(\rho_1, 0)$, the trajectory can be regarded as the system focus-saddle point solution. Figure 1. (b) corresponds to the first situation in Table 1. The system is unstable at the equilibrium point $(\rho_1, 0)$. When z→ $+\infty$, the spiral line tends to focus $(\rho_2, 0)$, the system is stable at this point; When z→ $-\infty$, away from the focus $(\rho_2, 0)$, the system is unstable at this point. The numerical results of phase planes in Figure 1(a) and Figure 1(b) are consistent with the theoretical analysis.

5 Conclusion

In this paper, traveling wave substitution is used to study the type and stability of equilibrium solutions of the improved Bando macro model. This paper selects two groups of parameters to describe the global distribution structure of the trajectory near the equilibrium point on the phase plane. Then, the stability of these equilibrium points is analyzed and described in detail. Finally, the results of the analysis are verified in the numerical simulation part, and the results are consistent with the theoretical derivation analysis.

The authors would like to thank the anonymous referees and the editor for their valuable opinions. This work is partially supported by the National Natural Science Foundation of China under the Grant No. 61863032 and the Natural Science Foundation of Gansu Province of China under the Grant No. 20JR5RA533 and the China Postdoctoral Science Foundation Funded Project (Project No.: 2018M633653XB) and the "Qizhi" Personnel Training Support Project of Lanzhou Institute of Technology (2018QZ-11) and Gansu Province Educational Research Project (Grant No. 2021A-166)

References

1. Goatin P, Rossi E. A Multilane Macroscopic Traffic Flow Model for Simple Networks[J]. Siam Journal on Applied Mathematics (S0036-1399), 2019, 79(5): 1967-1989
2. Michael H, Salissou M, Giuseppe V. Macroscopic Modeling of Multilane Motorways Using a Two-dimensional Second-order Model of Traffic Flow[J]. Siam Journal on Applied Mathematics (S0036-1399), 2018, 78(4): 2252-2278.
3. LI Li, JIANG Rui,JIA Bin,et al.Modern traffic flow theory and application: Volume 1,freeway traffic flow[M].Beijing: Tsinghua University Press,2011.(in Chinese)
4. M.J. Lighthill, G.B. Whitham. On kinematic waves. I. Flood movement in long rivers [J]. Proc. R. Soc. Lond. A, 1955, 229:281-316.
5. M.J. Lighthill, G.B. Whitham. On kinematic waves. II. A theory of traffic flow on long crowded roads[J], Proc. R. Soc. Lond. A, 1955, 229: 317-345.
6. Paul I. Richard, Shock waves on the highway, Oper. Res. 4 (1) (1956) 42–51.
7. M.Bando, K. Hasebe, A. Shibata, Y. Sugiyama. Dynamical model of traffic congestion and numerical simulation [J]. Phys. Rev. E, 1995, 51:1035-1042.
8. D. Helbing, B. Tilch. Generalized force model of traffic dynamics [J]. Phys. Rev. E, 1998, 58:133-138
9. Liu Huaqing. Traffic flow macro model modeling and congestion control analysis [D]. Ningbo University, 2016. (in Chinese)
10. B.S. Kerner, P. KonhÄauser. Cluster effect in initially homogeneous traffic flow [J]. Physical Review E, 1993, 48: 2335-2338.